Bonding Effects on the Slip Differences in the $B1$ Monocarbides

Nicholas De Leon,[1] Xiao-xiang Yu,[1] Hang Yu,[2] Christopher R. Weinberger,[2] and Gregory B. Thompson[1,*]
[1]Department of Metallurgical & Materials Engineering, The University of Alabama, Box 870202, Tuscaloosa, Alabama 35401-0202, USA
[2]Department of Mechanical Engineering and Mechanics, Drexel University, 3141 Chestnut Street, Philadelphia, Pennsylvania 19104, USA

(Received 16 January 2015; revised manuscript received 2 March 2015; published 24 April 2015)

Differences in plasticity are usually attributed to significant changes in crystalline symmetry or the strength of the interatomic bonds. In the $B1$ monocarbides, differences in slip planes exist at low temperatures despite having the same structure and very similar bonding characteristics. Our experimental results demonstrate concretely that HfC slips on $\{110\}$ planes while TaC slips on $\{111\}$ planes. Density functional theory calculations rationalize this difference through the formation of an intrinsic stacking fault on the $\{111\}$ planes, formation of Shockley partials, and enhanced metallic bonding because of the valence filling of electrons between these transitional metal carbides.

DOI: 10.1103/PhysRevLett.114.165502 PACS numbers: 62.20.fq, 31.15.ae, 71.15.Mb, 81.05.Je

Plasticity and ductility are generally associated with crystalline symmetry and the strength of the interatomic bonds [1]. For example, face centered cubic (FCC) and hexagonal close packed (HCP) materials have equivalent packing with similar types of bonding but show dramatic differences in deformation because of the availability of slip systems associated with their symmetry. Alternatively, dramatic differences in bonding, such as those between ceramics and metals, can also have a similar impact on dislocation slip and ductility, but such differences are confounded by variances in symmetry. What can be even more perplexing are materials that exhibit equivalent symmetry and bonding but show differences in deformation responses. In this Letter, we explore how a subtle difference in bonding behavior regulates the slip response in two equivalently structured and similarly bonded monocarbides by combining density functional theory (DFT) and experimental results. Our findings debunk how prior hard sphere based models are not able to rationalize experimental findings. Through the use of these modern computational tools, we elucidate how bonding, along with symmetry, regulates slip in this class of transition metal monocarbides (TMMCs).

The group IVB and VB monocarbides provide a perfect test bed to explore subtle differences in bonding and its role in mechanical properties. Both groups of TMMCs form the $B1$, or rocksalt structure, which is an array of FCC metal atoms with the carbon atoms filling every octahedral interstice [2,3]. The bonding in these materials is a mix of covalent, metallic, and ionic resulting in high hardness as well as good thermal and electrical conductivity [4–7]. The materials are generally brittle at room temperature and exhibit remarkable ductility at elevated temperatures [8–10].

The last comprehensive summary of plastic deformation of TMMCs was written by Rowcliffe in 1984 [11], where most slip systems were determined using hardness anisotropy. This work reported that the dominant slip systems in the group IVB monocarbides are $a/2\langle 110\rangle\{110\}$, while the group VB monocarbides revealed $a/2\langle 110\rangle\{111\}$ at room temperature. Rowcliffe *et al.* [12] also noted that the group IVB TMMCs were significantly more brittle than the group VB TMMCs, which is attributed to the number of available independent slip systems in the dominant family, i.e., two for the $a/2\langle 110\rangle\{110\}$ and five for $a/2\langle 110\rangle\{111\}$. The Supplemental Material of this Letter provides a review and summary table which shows both slip systems are found in all of the materials [13]. However, it has been established from past experiments [8,11,26–28] that one family of slip system appears to be dominant for each type of carbide, i.e., the $\{110\}$ in the group IVB TMMCs and $\{111\}$ in the group VB TMMCs. Though these differences have been known for decades, the change in slip systems across the TMMCs has perplexed scientists for equally as long.

To eliminate differences in homologous temperatures, we pick the two monocarbides with nearly equivalent melting temperatures, HfC($\sim$3900°C) and TaC($\sim$3880°C), to conduct our studies. The deformation of TaC has been well investigated across a number of temperatures establishing its preference to slip on $\{111\}$ planes through indentation experiments and elevated temperature creep studies [11,28]. Despite the well-known preference for slip on $\{111\}$ planes, the mechanism controlling slip is not well known. Authors have suggested a simple high lattice friction model with dislocations splitting into Shockley partials, a synchro-shear mechanism regulated by carbon diffusion, as well as motion via zonal dislocations to rationalize experimental observations [9,11,29], the latter two being unlikely to occur during room temperature deformation. In addition, as the carbon

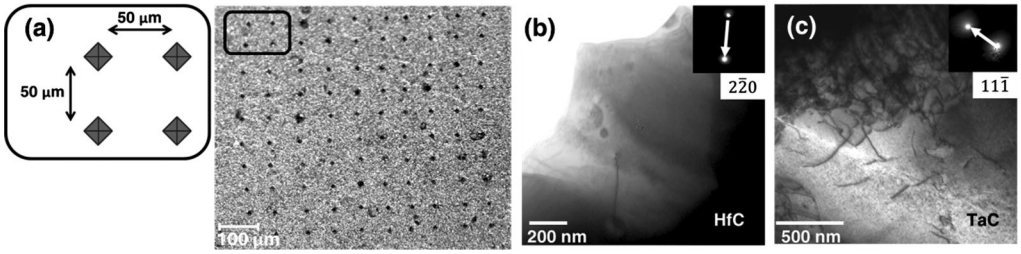

FIG. 1. (a) Representative schematic and optical micrograph of the 10×10 array of Vickers indents in a carbide specimen. TEM bright field micrographs of typical dislocation structures found in HfC (b) and TaC (c).

concentration in TaC_{1-x} is reduced, hardness anisotropy measurements indicated that $\{110\}$ slip becomes more prevalent [30]. In contrast, there have been limited studies in HfC and few theories that explain the $\{110\}$ slip in this system or other similar group IVB carbides. The typical explanation has been that these materials have more covalent bonding preventing $\{111\}$ slip [11,31]. As the temperature increases, one can expect that multiple slip systems would become more favorable and a dominate slip system, as noted in lower homologous temperatures, may not be as apparent.

To verify these results obtained decades ago, we performed microindentation tests, Fig. 1(a), in nearly stoichiometric HfC and TaC at room temperature with the corresponding dislocations observed in the TEM micrographs of Figs. 1(b) and 1(c). The TEM results confirm large amounts of dislocation plasticity within the TaC grains under the indents, whereas the plasticity in HfC was much more limited and confined to large grains directly under the indents with estimated dislocation densities being $\sim 1.10 \times 10^{14}$ m^{-2}(TaC) and $\sim 8.83 \times 10^{13}$ m^{-2}(HfC) under the indents and $\sim 1.32 \times 10^{14}$(TaC) and $\sim 3.12 \times 10^{11}$ m^{-2}(HfC) away from the indents; the experimental details can be found in the Supplemental Material [13].

Dynamical diffraction TEM analysis confirmed the slip system as $a/2\langle 110\rangle\{111\}$ in TaC and $a/2\langle 110\rangle\{110\}$ in HfC [13]. LECO analysis confirmed nearly stoichiometric and equal amounts of carbon in the samples, eliminating this as a cause for the change in slip planes. These results, in addition to the previous observations in single crystals [12], suggest the choice of slip planes and the limited ductility in HfC compared to TaC are intrinsic properties.

It is generally thought that slip will occur in the close-packed directions on the most widely spaced planes This suggests slip on $\{111\}$ planes in FCC metals and the $\{110\}$ slip in BCC metals and is thought to control the competition between basal and prism slip in HCP metals. The other factor complicating slip is the existence of fault planes [32]. However, this can be complicated in materials with mixed bonding. The predominately held belief with regard to the differences in slip for group IVB and VB carbides was based on the hard sphere model. First proposed to be viable in ionic and covalent materials by Van Der Walt and Sole [33], Rowcliffe and Hollox [30] supported its applicability to carbides. The hard sphere model relates preferred slip to the interatomic spacing within the structure as determined by the ratio of the radii of the carbon and metal atoms. It states that perfect slip on the $\{110\}$ plane is preferred in covalently bonded materials with a radius ratio $(r/R) < 0.414$, on the $\{111\}$ plane when $0.414 \leq r/R \leq 0.633$, and on the $\{100\}$ when $r/R > 0.633$. It also only predicts partial slip on the $\{111\}$ plane at $r/R > 0.732$. The radius ratios of all the group IVB and VB carbides, as reported by Toth [4], along with the hard sphere model slip predictions and the experimentally reported and observed active slip systems are tabulated in the Supplemental Material [13] for the reader. These results suggest that all of the TMMCs should deform via the $\{111\}$ slip despite the observations of the $\{110\}$ slip dominance in the group IVB TMMCs. Given the close radius ratio between TiC and the group VB TMMCs, the model has difficulty even predicting trends. It is evident that the hard sphere model does not adequately explain or predict favorable slip within the TMMCs even though it has been propagated for several years in contrast to prior experimental data. Moreover, it further breaks down when partial slip is added to the discussion as will be elucidated shortly.

To provide for a more accurate understanding of slip, we have employed first-principles DFT calculations of the generalized stacking fault (GSF) energies (see Supplemental Material [13]). The GSF energy surfaces for perfect slip for the $\{110\}$ and $\{111\}$ planes are plotted in Fig. 2(a). It was found that in either TMMC system, $\{110\}$ slip was more energetically favorable than $\{111\}$ when compared along the $\langle 110\rangle$ direction. Moreover TaC was shown to have a lower GSF than HfC, which helps explain the higher dislocation densities noted in the material between the two carbides, Fig. 1. Though TaC has a lower GSF energy than HfC, this does not explain its dominance on $\{111\}$ planes, as perfect slip on these planes are nearly twofold higher in energy than the $\{110\}$ perfect slip, Fig. 2(a). The choice of slip planes rather lies with the presence of an intrinsic fault, Fig. 2(b), and ability of the perfect dislocations to split into Shockley partials, Figs. 2(c) and 2(d).

It is well known that dislocations in close-packed metals, amongst others, dissociate into partial dislocations

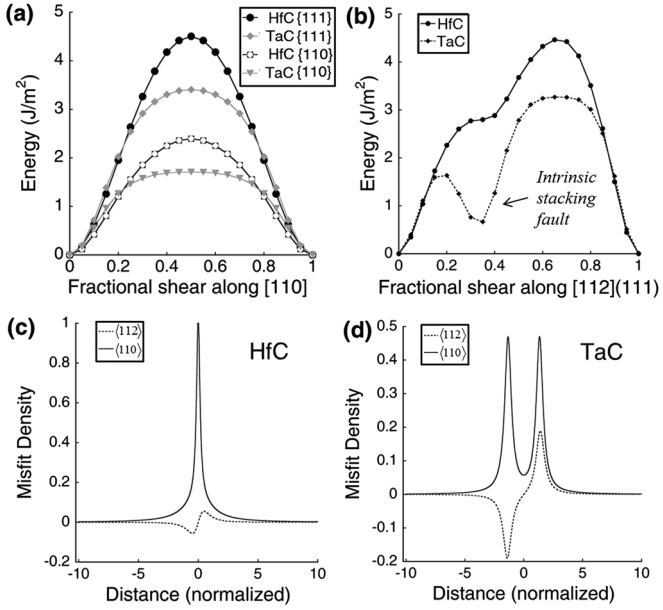

FIG. 2. DFT calculated generalized stacking fault energy curves for fractional shear along (a) [110] on both the (111) and (110) planes and (b) for the partial dissociation [112] (111) for both HfC and TaC. Note the intrinsic stacking fault in TaC which is absent in HfC. Associated PN model misfit density plots for (c) HfC and (d) TaC, with the distance normalized by the Burgers vector. The preference for splitting into partials is evident in TaC and not HfC.

to reduce the elastic energy of the system [20]. To explore this possibility in the TMMCs, we computed the $\langle 112\rangle\{111\}$GSF curves for HfC and TaC, Fig. 2(b). In this configuration a local 1D minima in TaC, known as an intrinsic stacking fault (ISF), is noted but is absent in HfC. This ISF was noted to be present in all of the group VB TMMCs but absent in the group IVB TMMCs (see Supplemental Material) [13], indicating uniformity across the two family classes of monocarbides [13]. The ISF, when present, represents a metastable minimum energy configuration in the energy surface, which may result in the splitting of perfect dislocations into partial dislocations. The unstable stacking fault energy (USF) is the maximum energy along the minimum energy path and can indicate the relative ductility of a material [34,35]. In the hard sphere model, an ISF is only present for radius ratios or $r/R > 0.732$, when the hard sphere model predicts the $\{001\}$ slip. The presence of an ISF in TaC, which would correspond to the $\{001\}$ slip in the hard sphere model, is a direct indication of a fundamental breakdown of the hard sphere model. Moreover, the presence of a stable ISF also likely contributes to the phase stability of faulted phases, such as Ta_4C_3, in substoichiometric tantalum carbides but such phases are not observed in the hafnium carbides [36].

These DFT calculations shed new light into the differences in the room-temperature slip behavior between the two carbides that has been lacking for years. Perfect slip on the $\{110\}$ surface is energetically most favorable for HfC, which is in agreement with the results reported here and elsewhere [11]. In contrast, TaC can supersede the $\{110\}$ slip because of its favorable ISF on the $\{111\}$ plane, which is absent in HfC.

To confirm that dislocations dissociate into partials in TaC on the $\{111\}$ plane, we used a Peierls-Nabarro (PN) model to compute the potential for dislocation dissociation. These results are shown in Figs. 2(c) and 2(d) and confirm our expectations based on the GSF curves alone. A TaC dislocation will split slightly into partial dislocations on the $\{111\}$ plane as shown by the separate peaks in Fig. 2(d). In contrast, the lack of the ISF prevents dislocations from splitting in HfC, also confirmed by our PN model in Fig. 2(c). Hence, the dissociation of the dislocations helps stabilize them on the $\{111\}$ plane and generally lowers their barrier to motion, making the $\{111\}$ slip more prevalent in TaC than HfC.

To fully understand how the DFT calculations can provide an alternate explanation to the hard sphere model concepts, one must consider the nature and directionality of the bonding within the carbides. Figure 3 shows the isoconcentration charge surfaces computed from our DFT simulations, providing a visual aid in highlighting the differences in the bonding between the carbides during the shear process. In all renderings, the isocharge surfaces were equivalent for direct visual comparison purposes [13]; see the Supplemental Material for details.

In the unsheared state, we can clearly see a difference the bonding that occurs in these two carbides. Notably, the isocharge surfaces are more diffuse between the atoms in TaC than in HfC regardless of the isocharge value used in the visualization. This indicates a less directional bond and thus more metalliclike character. This is a direct consequence of the extra valence electron contributed by tantalum, a group VB transition metal atom, to the Ta-C bond. The difference in bonding is further highlighted as the crystal shears, with the bonding behaving in a more localized fashion in HfC than TaC; i.e., compare the charge distribution between the two shear planes (dashed arrows) for the 0.5 shear along the $\langle 110\rangle\{110\}$.

The less directional nature of the bonds in TaC also allows for the stabilization of the ISF. The isocharge surfaces at a fractional shear of 0.35 in the $a/6\langle 112\rangle$ direction on the $\{111\}$ planes, Fig. 3, exhibit a rotation of the bonds for both TaC and HfC. As the top half of the crystal shears relative to the bottom half via a Shockley partial dislocation, the bonds between the metal atoms and carbon atoms in this plane undergo a 60° rotation about the plane normal. This bonding rotation increases the bond energy which will be a function of the angular nature of the bonds themselves. The less directional nature of the Ta-C bonds helps to mitigate the energy penalty for this bond rotation. Clearly, the extra d-shell valance electron of tantalum dramatically helps to stabilize the fault as

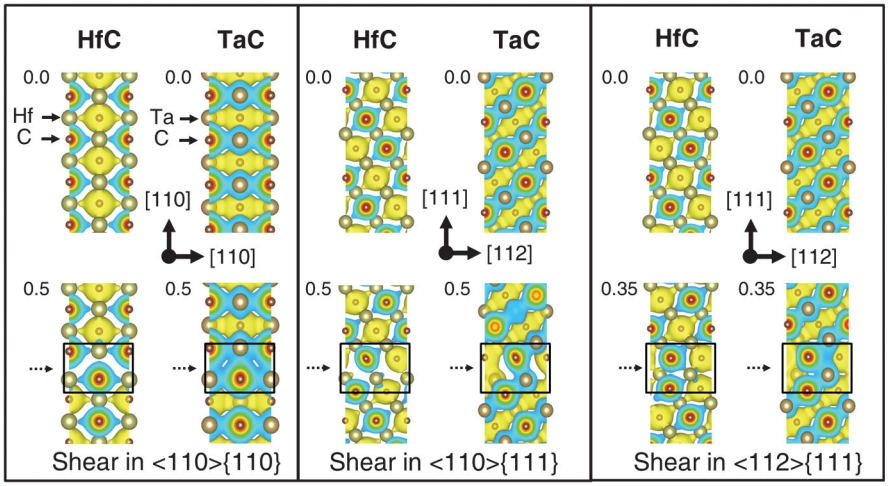

FIG. 3 (color). DFT isoconcentration charge surfaces for HfC and TaC in a zero and fraction shear state for various slip conditions. The dashed arrow indicates the fault plane highlighted by the solid box region. The top row shows the unsheared conditions with the bottom row being the designated shear indicated by the fraction value. The compass arrows indicate the viewing prospective.

compared to hafnium. Since both systems have equivalent coordination environments (bond hybridization), the extra *d* valance electron provides for some charge delocalization upon rotation and would explain the universality for a stabilized ISF in all of the other group VB TMMCs shown in the Supplemental Material [13].

This faulted configuration stacks the metal atoms over the metal atoms and the carbon atoms over the carbon atoms across the fault. In other words, the atoms directly in the fault have a trigonal prismatic coordination with respect to the other species and tetrahedral coordination with respect to their own atom type. It has been previously suggested that in the synchro-shear mechanism [29,37,38], the tetrahedral coordination of the metal atoms would be unfavorable. This would be correct for HfC but not necessarily true for TaC, where an ISF is favorable because of the nature of its bonds. Finally, it is interesting to note that their appears to be some bonding between carbon atoms in the TaC ISF though this is likely an artifact to the sensitivity of the exact isocharge value used in visualization. Similar stabilization of ISF energies has been noted with metallic alloys where the solute atoms contribute excess valence electrons to the system [39].

In summary, a series of room temperature indents in HfC and TaC were characterized using TEM dynamical diffraction analysis to determine the operating slip planes in these materials. We confirmed that $a/2\langle 110\rangle\{110\}$ slip occurs in HfC and $a/2\langle 110\rangle\{111\}$ slip in TaC at room temperature, with 2 orders of magnitude higher density of dislocations observed in TaC than HfC. Using DFT, the GSF curves for the $\{110\}$ and $\{111\}$ slip were computed revealing that the perfect $\{110\}$ slip was more favorable with TaC having a lower energy for slip than HfC. This result confirmed the dominant slip system observed in HfC and the higher dislocation density seen in TaC for equivalent room temperature indents. The presence of an ISF in TaC promotes the dissociation of perfect dislocations into partials on the $\{111\}$ plane, which allowed it to bypass the $\{110\}$ slip. The extra electron in TaC as compared to HfC provides a more metallic nature to the bonds [6,7], enhancing slip and stabilizing the ISF. Coupling prior experimental work in the other group IVB and VB TMMCs where different dominate slips planes have been reported [11,26–28] with their similar GSF curves (see Supplemental Material [13]), we have concluded that the slip variation is likely contributed to the ability to or not to form an ISF. The stability of this ISF appears to be related to the excess *d*-shell electron between these two groups of TMMCs. The operation of the $\{111\}$ slip allows for a larger number independent slip systems (i.e., 5) compared to the $\{110\}$ slip (i.e., 2), further enhancing the ductility of the material and changing its macroscopic properties. This suggests that engineering the stacking fault energy to access or limit specific deformation modes through solute alloying could allow for the future design of tunable hardness in these carbides beyond using simple elastic constant criteria [40–42].

This research was supported under the Air Force Office of Scientific Research under Grant No. FA9550-12-1-0104 DEF, Dr. Ali Sayir Program Manager; the Central Analytical Facility supported by The University of Alabama Office for Research; and, lastly, the high performance computing resources and technical support from the Alabama Supercomputer Authority is recognized.

*To whom all correspondence should be addressed.
gthompson@eng.ua.edu

[1] G. E. Dieter and D. Bacon, *Mechanical Metallurgy*, 3rd ed. (McGraw-Hill, New York, 1986).

[2] E. K. Storms, *The Refractory Carbides* (Academic Press, New York, 1967).
[3] G. Santoro and H. B. Probst, in *Advances in X-ray Analysis: Proceedings of the 12th Annual Conference on Applications of X-ray Analysis*, edited by W. M. Mueller, G. Mallett, and M. Fay (Plenum Press, New York, 1963).
[4] L. E. Toth, *Transition Metal Carbides and Nitrides* (Academic Press, New York, 1971).
[5] W. S. Williams, Prog. Solid State Chem. **6**, 57 (1971).
[6] F. Viñes, C. Sousa, P. Liu, J. A. Rodriguez, and F. Illas, J. Chem. Phys. **122**, 174709 (2005).
[7] Y. Liu, Y. Jiang, R. Zhou, and J. Feng, J. Alloys Compd. **582**, 500 (2014).
[8] A. Kelly and D. J. Rowcliffe, J. Am. Ceram. Soc. **50**, 253 (1967).
[9] G. E. Hollox, Mater. Sci. Eng. **3**, 121 (1968).
[10] R. Steinitz, in *Conference on Nuclear Applications of Nonfissionable Ceramics*, edited by A. Boltax and J. H. Handwerk (American Nuclear Society, Washington, DC, 1966), p. 75.
[11] D. J. Rowcliffe, in *Deformation of Ceramic Materials II*, edited by R. Tressler and R. Bradt (Springer, New York, 1984), p. 49.
[12] D. J. Rowcliffe and G. E. Hollox, J. Mater. Sci. **6**, 1261 (1971).
[13] See Supplemental Material at http://link.aps.org/supplemental/10.1103/PhysRevLett.114.165502 for detailed methodology and additional results, which includes Refs. [14–25].
[14] Northern Analytical Laboratory. [LECO testing results]. Unpublished raw data (2013) edited by N. A. Laboratories13 Delta Drive #4 Londonderry, NH 03053.
[15] E. Rudy and D. P. Harmon, Report No. AFML-TR-65-2, Part I, Volume V (Air Force Materials Laboratory Research and Technology Division, Air Force Command, Wright-Patterson A.F.B., Ohio, 1965).
[16] G. Ravichandran and G. Subhash, Int. J. Solids Struct. **32**, 2627 (1995).
[17] J. W. Edington, *Practical Electron Microscopy in Materials Science* (N.V. Philips' Gloeilampenfabrieken, Eindhoven, 1976).
[18] R. K. Ham, Philos. Mag. **6**, 1183 (1961).
[19] F. R. Castro-Fernáandez and C. M. Sellars, Philos. Mag. A **60**, 487 (1989).
[20] P. E. Blöchl, Phys. Rev. B **50**, 17953 (1994).
[21] G. Kresse and J. Furthmüller, Phys. Rev. B **54**, 11169 (1996).
[22] J. P. Perdew, K. Burke, and M. Ernzerhof, Phys. Rev. Lett. **77**, 3865 (1996).
[23] A. L. Bowman, J. Phys. Chem. **65**, 1596 (1961).
[24] P. Villars and L. D. Calvert, *Pearson's Handbook of Crystallographic Data for Intermetallic Phases* (American Society for Metals, Metals Park, OH, 1985), Vol. 2.
[25] V. V. Bulatov and W. Cai, *Computer Simulations of Dislocations, Oxford Series on Materials Modelling: 3* (Oxford University Press, Oxford, 2006).
[26] D. W. Lee and J. S. Haggerty, J. Am. Ceram. Soc. **52**, 641 (1969).
[27] G. Morgan and M. H. Lewis, J. Mater. Sci. **9**, 349 (1974).
[28] C. Kim, G. Gottstein, and D. S. Grummon, Acta Metall. Mater. **42**, 2291 (1994).
[29] M. H. Lewis, J. Billingham, and P. S. Bell, in *Electron Microscopy and Structure of Materials, Proceedings of the 5th International Materials Symposium*, edited by G. Thomas, R. Fulrath, and R. M. Fisher (University of California, Berkeley, 1971), p. 1084.
[30] D. J. Rowcliffe and G. E. Hollox, J. Mater. Sci. **6**, 1270 (1971).
[31] R. H. J. Hannink, D. L. Kohlstedt, and M. J. Murray, Proc. R. Soc. A **326**, 409 (1972).
[32] J. P. Hirth and J. Lothe, *Theory of Dislocations* (Krieger, Malabar, 1982).
[33] C. M. Van Der Walt and M. J. Sole, Acta Metall. **15**, 459 (1967).
[34] J. R. Rice and G. E. Beltz, J. Mech. Phys. Solids **42**, 333 (1994).
[35] S. Ogata, J. Li, N. Hirosaki, Y. Shibutani, and S. Yip, Phys. Rev. B **70**, 104104 (2004).
[36] X. X. Yu, C. R. Weinberger, and G. B. Thompson, Acta Mater. **80**, 341 (2014).
[37] J. Hornstra, J. Phys. Chem. Solids **15**, 311 (1960).
[38] M. L. Kronberg, Acta Metall. **5**, 507 (1957).
[39] X. X. Yu and C. Y. Wang, Acta Mater. **57**, 5914 (2009).
[40] H. Li, L. Zhang, Q. Zeng, H. Ren, K. Guan, Q. Liu, and L. Cheng, Solid State Commun. **151**, 61 (2011).
[41] D. Varshney, S. Shriya, and N. Singh, *AIP Conf. Proc.* 1512, 1016 (2013).
[42] X. X. Yu, G. B. Thompson, and C. R. Weinberger, J. Eur. Ceram. Soc. **35**, 95 (2015).